J. Fluid Mech. (1985), *vol.* 161, *pp.* 295–312
Printed in Great Britain

Linear and nonlinear stability of plane stagnation flow

By M. J. LYELL AND P. HUERRE
Department of Aerospace Engineering, University of Southern California, Los Angeles, California 90089-0192

(Received 28 June 1985)

Plane stagnation flow is known to be linearly stable to three-dimensional perturbations. The purpose of this theoretical study is to show that the same flow can be destabilized if fluctuation levels are sufficiently high. In the present formulation, finite-amplitude disturbances are expanded in terms of the eigenfunctions pertaining to the linear stability of potential stagnation flow and a Galerkin method is used to derive the nonlinear amplitude equations coupling the different modes. Two- and three-mode interaction models based on the least-damped eigenfunctions of linear theory indicate that three-dimensional fluctuations can be triggered to grow exponentially above a certain critical intensity. The existence of such a threshold is in qualitative agreement with experimental studies of the secondary vortices arising in flows past blunt bodies.

1. Introduction

It is known from experimental observations that steady or unsteady streamwise vortices may be formed in the stagnation region of flows past bluff bodies. Piercy & Richardson (1928) were the first to detect the presence of large unsteady velocity fluctuations in the stagnation-flow region of bluff bodies. More recent investigations by Sadeh, Sutera & Maeder (1970), Colak-Antic (1971), Hassler (1971), Hodson & Nagib (1975) and Sadeh & Brauer (1980), among others, have revealed a wealth of possible secondary-flow regimes. Applications of stability theory to viscous plane stagnation flow have been mainly motivated by the need to understand this peculiar phenomenon. For a comprehensive and critical account of this class of instabilities, the reader is referred to the review by Morkovin (1979).

The presence, in the plane-viscous-stagnation-flow region, of mean flow vorticity and concave streamline curvature led Görtler (1955) and Hämmerlin (1955) to suspect that the secondary vortices might be the result of a centrifugal instability mechanism. The geometry of the flow considered by these authors is as sketched in figure 1 and their linear stability analysis is essentially contained in (7) and (8) of §3, where the growth rate σ was set identically equal to zero. The three-dimensional perturbations of spanwise wavenumber k, which satisfy system (8), were required by Görtler and Hämmerlin to decay *algebraically* at upstream infinity. This asymptotic boundary condition leads to a *continuous* spectrum of spanwise wavenumbers, $0 < k < 1$, with no clear conclusion as to the stable or unstable nature of viscous plane stagnation flow.

The work of Wilson & Gladwell (1978) has now considerably clarified the issue of the 'correct' asymptotic boundary condition at upstream infinity. If disturbances are to be viewed as originating in the viscous-stagnation-flow region, they must decay

exponentially far upstream. Such a condition then leads to a discrete spectrum of eigenvalues $\sigma(k)$, none of which are positive. Thus the conclusion of Wilson & Gladwell (1978) is that viscous stagnation flow is linearly stable to three-dimensional disturbances of the form given by (7). In contrast with this situation, vortical disturbances forced from the outer potential mean flow will experience algebraic growth or decay as they enter the viscous layer; they correspond, in the linear theory, to the continuous spectrum of Görtler and Hämmerlin.

An extension of Görtler and Hämmerlin's linear results to small-but-finite amplitude perturbations has been proposed by Iida (1978). The weakly nonlinear formalism of Stuart (1960) and Watson (1960) is used to derive an amplitude equation governing the evolution of fluctuations. It should be emphasized that such an approach is only valid in the neighbourhood of a neutral stability boundary, say, in the wavenumber–Reynolds-number plane. But viscous plane stagnation flow is a self-similar solution of the Navier–Stokes equations in which the Reynolds number does not appear as an independent parameter. The flow is linearly stable and there is no neutral curve. This is in contrast to the related flow situation of a boundary layer over a curved plate, in which the Görtler number serves as the independent parameter (see, for example, Hall 1982, 1983). The case of plane stagnation flow is then qualitatively similar to the case of pipe flow that is linearly stable at all Reynolds numbers. The weakly nonlinear approach does not seem to be applicable to this class of problems.

To analyse the linear and nonlinear stability problems, we choose instead a Galerkin expansion method which does not require for its application the existence of a neutral stability boundary. The basic formalism is given in §2. The linear and nonlinear stability of stagnation flow are discussed respectively in §§3 and 4. The results are presented in §5.

2. Basic formulation

We consider an infinite flat plate oriented normal to the direction of an initially uniform stream. The geometry of the flow and the coordinate system are indicated in figure 1. The flat plate is in the (x, z)-plane and the basic flow is two-dimensional in the (x, y)-plane, the x-axis being the streamwise direction along the plate, and the z-axis the spanwise direction. The stagnation streamline coincides with the y-axis. The spatial coordinates x, y, z, the time t, and all the dependent flow variables have already been made non-dimensional with respect to the upstream velocity V_∞ and the boundary-layer thickness δ. In addition, let

$$X = \frac{x}{R}, \quad T = \frac{t}{R} \tag{1}$$

denote rescaled x- and t-coordinates, R being the Reynolds number based on δ and V_∞.

The total velocity components U, V, W along the x-, y- and z-directions, and the pressure P are then assumed to be in the separable form

$$U(X, y, z, T) = XF'(y) + X\hat{u}(y, z, T), \tag{2a}$$

$$V(X, y, z, T) = -\frac{1}{R}F(y) + \frac{1}{R}\hat{v}(y, z, T), \tag{2b}$$

$$W(X, y, z, T) = \frac{1}{R}\hat{w}(y, z, T), \tag{2c}$$

$$P(X, y, z, T) = -\tfrac{1}{2}X^2 + \frac{1}{R^2}G(y) + \frac{1}{R^2}\hat{p}(y, z, T), \tag{2d}$$

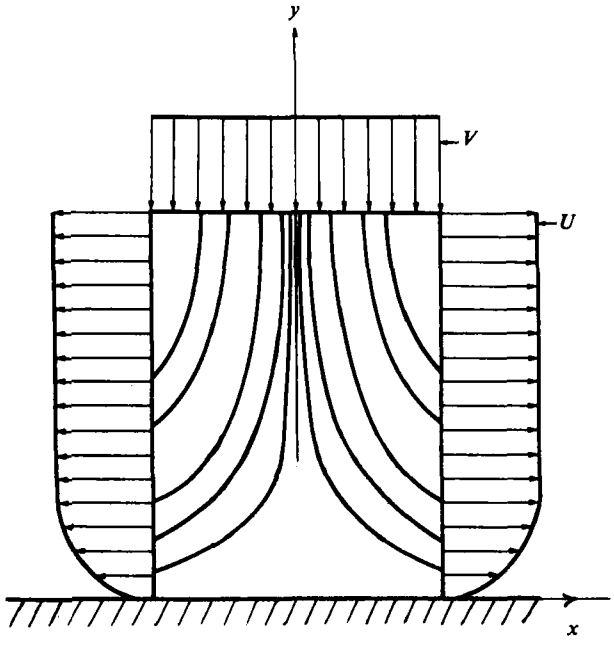

FIGURE 1. Hiemenz two-dimensional stagnation flow.

where the stream function of the basic flow is $XF(y)$. The three-dimensional fluctuations are indicated by a caret. The basic flow is taken to be the exact Hiemenz solution of the two-dimensional Navier–Stokes equations (see Schlichting 1979). Substitution of the decomposition (2) into the Navier–Stokes equations yields the nonlinear perturbation equations

$$\left[\frac{\partial}{\partial T}-F\frac{\partial}{\partial y}+2F'-\frac{\partial^2}{\partial y^2}-\frac{\partial^2}{\partial z^2}\right]\hat{u}+F''\hat{v}=-\left(\hat{u}+\hat{v}\frac{\partial}{\partial y}+\hat{w}\frac{\partial}{\partial z}\right)\hat{u}, \tag{3a}$$

$$\left[\frac{\partial}{\partial T}-F\frac{\partial}{\partial y}-F'-\frac{\partial^2}{\partial y^2}-\frac{\partial^2}{\partial z^2}\right]\hat{\omega}=\left(\hat{u}-\hat{v}\frac{\partial}{\partial y}-\hat{w}\frac{\partial}{\partial z}\right)\hat{\omega}, \tag{3b}$$

$$\hat{u}+\frac{\partial\hat{v}}{\partial y}+\frac{\partial\hat{w}}{\partial z}=0, \tag{3c}$$

$$\frac{\partial\hat{w}}{\partial y}-\frac{\partial\hat{v}}{\partial z}=\hat{\omega}. \tag{3d}$$

Note that the X-dependence of the flow variables has been explicitly separated according to (2); system (3) is composed of partial differential equations in y, z and T only. Equation (3*b*) governs the evolution of the streamwise perturbation-vorticity component ω defined in (3*d*). It has been obtained by eliminating the pressure from the original equations. Disturbances are required to decay exponentially at $y=\infty$ and the no-slip boundary conditions

$$\hat{u}(0,z,T)=\hat{v}(0,z,T)=\hat{w}(0,z,T)=0 \tag{3e}$$

are imposed on the surface of the plate.

In the present work, a Galerkin method (DiPrima 1967; Finlayson 1972) is

implemented to study both the linear and nonlinear stability problems. Thus we assume general expansions of the form

$$\hat{u}(y,z,T) = \sum_{m=1}^{\infty} A_{0m}^{(1)}(T)\, u_{0m}^{(1)}(y) + \sum_{n=1}^{\infty}\sum_{m=1}^{\infty} \{A_{nm}^{(1)}(T)\, u_{nm}^{(1)}(y)\cos(nqz) + A_{nm}^{(2)}(T)\, u_{nm}^{(2)}(y)\sin(nqz)\}, \quad (4a)$$

$$\hat{\omega}(y,z,T) = \sum_{m=1}^{\infty} A_{0m}^{(2)}(T)\, \omega_{0m}^{(2)}(y) + \sum_{n=1}^{\infty}\sum_{m=1}^{\infty} \{A_{nm}^{(1)}(T)\, \omega_{nm}^{(1)}(y)\sin(nqz) + A_{nm}^{(2)}(T)\, \omega_{nm}^{(2)}(y)\cos(nqz)\}, \quad (4b)$$

where the subscript n indicates the order of the spanwise harmonic $k = nq$, and the subscript m the mth trial function. In other words, disturbances are taken to be periodic in the spanwise z-direction, of wavelength $2\pi/q$. The expansion for v and w are of the same form as u and ω respectively.

The amplitude functions $\{A_{nm}^{(j)}(T)\}$ are at this stage unknown, and the infinite set of trial function vectors $\boldsymbol{U}_{nm}^{(j)\mathrm{T}} = \{u_{nm}^{(j)}, \omega_{nm}^{(j)}, v_{nm}^{(j)}, w_{nm}^{(j)}\}$ must be selected so as to satisfy the boundary conditions at $y = 0$ and $y = \infty$. The linear eigenfunctions of Hiemenz flow, calculated by Wilson & Gladwell (1978), do meet these requirements. However, higher eigenvalue branches are unknown and their determination would require extensive numerical calculations. In this study, we prefer to choose trial functions that not only satisfy all the boundary conditions, but also can be entirely derived analytically, namely the linear eigenfunctions pertaining to the stability of potential stagnation flow $F(y) = y$ (see §3.1).

The goal of the Galerkin method is then to generate a system of nonlinear ordinary differential equations describing the evolution of the modal amplitude functions $\{A_{nm}^{(j)}(T)\}$. To this end, the following methodology is employed. Expansion (4) is first substituted into the full nonlinear equations (3), and coefficients of $\cos(nqz)$ and $\sin(nqz)$ are separately equated to yield an infinite set of coupled equations for the vectors $\boldsymbol{U}_{nm}^{(j)}(y)$. We then take the inner product, defined as

$$\langle U, \tilde{U}\rangle = \int_0^{\infty} (u\tilde{u} + v\tilde{v} + w\tilde{w} + \omega\tilde{\omega})\,\mathrm{d}y, \quad (5)$$

of each resulting equation with the adjoint trial-function vector $\tilde{\boldsymbol{U}}_{nm}^{(j)}(y)$ to obtain the system of nonlinear evolution equations:

$$\frac{\mathrm{d}A_{nm}^{(j)}}{\mathrm{d}T} = \sum_{r=1}^{\infty} (\alpha_{nmr}\, A_{nr}^{(j)}) + Q_{nm}^{(j)}[A_{rs}^{(l)}], \quad (6)$$

where $n = 1, 2, \ldots$, $m = 1, 2, \ldots$, and $j = 1, 2$. The functions $Q_{nm}^{(j)}$ are quadratic forms in the modal amplitudes $A_{rs}^{(l)}$. At small amplitudes, these quadratic terms are negligible and all harmonic components decouple from each other. For a given wavenumber $k = nq$, an infinite set of linear ordinary differential equations is then obtained and the eigenvalues of the matrix $\{\alpha_{nmr}\}$, n fixed, coincide with the linear growth rates of viscous stagnation flow evaluated at $k = nq$.

3. Linear stability of plane stagnation flow

In this section, we first determine analytically the viscous linear stability characteristics of potential stagnation flow $F = y$. The associated eigenfunctions are then used as trial functions to determine via the Galerkin method the stability properties of Hiemenz stagnation flow. The same set of trial functions is chosen in the nonlinear stability analysis. Since Hiemenz flow reduces to potential flow in the limit $y \to \infty$, the asymptotic behaviour of the eigenfunctions at large y will be the same for both basic flows. Furthermore, while the basic potential flow allows slip on the plate $y = 0$, no-slip boundary conditions are enforced on the fluctuations. Thus the eigenfunctions of $F = y$, which satisfy the same boundary conditions as those of Hiemenz flow, are ideally suited to constitute a set of trial functions in the Galerkin expansion (4). As shown in §3.3, this selection of trial functions serves to elucidate the structure of the perturbed flow field.

In *linearized analyses* of viscous stagnation flow, the nonlinear terms on the right-hand side of system (3) are neglected and the perturbation quantities are further assumed to be of the form

$$\hat{u}(y,z,T) = \{u^{(1)}(y;k)\cos kz + u^{(2)}(y;k)\sin kz\}\,\mathrm{e}^{\sigma(k)T}, \tag{7a}$$

$$\hat{\omega}(y,z,T) = \{\omega^{(1)}(y;k)\sin kz + \omega^{(2)}(y;k)\cos kz\}\,\mathrm{e}^{\sigma(k)T}, \tag{7b}$$

$$\hat{v}(y,z,T) = \{v^{(1)}(y;k)\cos kz + v^{(2)}(y;k)\sin kz\}\,\mathrm{e}^{\sigma(k)T}, \tag{7c}$$

$$\hat{w}(y,z,T) = \{w^{(1)}(y;k)\sin kz + w^{(2)}(y;k)\cos kz\}\,\mathrm{e}^{\sigma(k)T}, \tag{7d}$$

where k denotes the spanwise wavenumber and σ the temporal growth rate. The governing equations pertaining to variables with a (1) superscript then reduce to the following ordinary differential equations

$$\left[\frac{\mathrm{d}^2}{\mathrm{d}y^2} + F\frac{\mathrm{d}}{\mathrm{d}y} + \nu - 2F'\right]u^{(1)} - F''v^{(1)} = 0, \tag{8a}$$

$$\left[\frac{\mathrm{d}^2}{\mathrm{d}y^2} + F\frac{\mathrm{d}}{\mathrm{d}y} + \nu + F'\right]\omega^{(1)} = 0, \tag{8b}$$

$$u^{(1)} + \frac{\mathrm{d}v^{(1)}}{\mathrm{d}y} + kw^{(1)} = 0, \tag{8c}$$

$$\frac{\mathrm{d}w^{(1)}}{\mathrm{d}y} + kv^{(1)} = \omega^{(1)}, \tag{8d}$$

with exponentially decaying boundary conditions at $y = \infty$ and

$$u^{(1)}(0;k) = v^{(1)}(0;k) = w^{(1)}(0;k) = 0. \tag{8e}$$

The above system defines an eigenvalue problem for the auxiliary parameter $\nu(k) = -\sigma(k) - k^2$, and the solution vector $\boldsymbol{U}^{(1)\mathrm{T}}(y;k) \equiv \{u^{(1)}, \omega^{(1)}, v^{(1)}, w^{(1)}\}$. The variables denoted by a superscript (2) satisfy the same equations and boundary conditions, provided that w and ω are changed in sign. The growth rates $\sigma^{(1)}(k)$ and $\sigma^{(2)}(k)$ are therefore identical, as already anticipated in decomposition (7), where we have set $\sigma^{(1)}(k) = \sigma^{(2)}(k) \equiv \sigma(k)$. Furthermore, the direct numerical integration of system (8) performed by Wilson & Gladwell (1978) has indicated that the eigenvalues of the least-damped branch $\sigma_1(k)$ are negative for all k, which implies that Hiemenz flow is linearly stable.

3.1. *Linear stability of potential stagnation flow*

When $k \neq 0$, the solution of the linear system (8), with $F \equiv y$, can be expressed in terms of parabolic cylinder functions $D\mu(y)$. After excluding algebraically growing or decaying solutions at $y = \infty$, and imposing the boundary conditions at $y = 0$, one obtains the dispersion relation

$$\int_0^\infty \mathrm{e}^{-kt-\frac{1}{4}t^2} D_\nu(t)\,\mathrm{d}t \cdot D_{\nu-3}(0) = 0 \tag{9}$$

for the eigenvalues $\{\nu_m(k)\}$, $m = 1, 2, 3, \ldots$. When the first and second factor are individually set equal to zero, one obtains two distinct families which are respectively denumerated by odd and even subscripts. The integral expression in (9) has an infinite number of roots $\{\nu_{2p-1}(k)\}$, $p = 1, 2, 3, \ldots$, which must be determined numerically. The even-numbered eigenvalues, defined as the zeroes of $D_{\nu-3}(0)$, take the simple form

$$\nu_{2p-2}(k) = 2p, \quad p = 2, 3, \ldots. \tag{10}$$

Thus there is a double infinity of eigenvalues $\{\nu_{2p-1}(k)\}$, $\{\nu_{2p-2}(k)\}$ or, equivalently, $\{\sigma_{2p-1}(k)\}, \{\sigma_{2p-2}(k)\}$, the variations of the first few branches with wavenumber k being shown in figures 2 and 3. With the exception of the least-damped mode $\sigma_1(k)$, eigenvalues occur in even and odd pairs. Note, however, that our indexing scheme for m does not order successive branches in terms of monotonically decreasing values of σ. Growth rates σ are found to be negative for all values of k and all branches, indicating that potential stagnation flow is linearly stable. The components of the eigenvectors $\boldsymbol{U}_m^{(1)}(y; k)$ pertaining to the odd-numbered and even-numbered families are, respectively,

$$u_{2p-1}^{(1)}(y; k) = 0, \tag{11a}$$

$$\omega_{2p-1}^{(1)}(y; k) = \mathrm{e}^{-\frac{1}{4}y^2} \frac{D_{\nu_{2p-1}}(y)}{D_{\nu_{2p-1}}(0)}, \tag{11b}$$

$$v_{2p-1}^{(1)}(y; k) = \frac{1}{D_{\nu_{2p-1}}(0)} \int_y^\infty \mathrm{e}^{-\frac{1}{4}t^2} D_{\nu_{2p-1}}(t) \sinh\left(k(y-t)\right) \mathrm{d}t + \gamma_{2p-1}(k)\,\mathrm{e}^{-ky}, \tag{11c}$$

$$w_{2p-1}^{(1)}(y; k) = -\frac{1}{D_{\nu_{2p-1}}(0)} \int_y^\infty \mathrm{e}^{-\frac{1}{4}t^2} D_{\nu_{2p-1}}(t) \cosh\left(k(y-t)\right) \mathrm{d}t + \gamma_{2p-1}(k)\,\mathrm{e}^{-ky}, \tag{11d}$$

and

$$u_{2p-2}^{(1)}(y; k) = \beta_{2p-2}(k)\,\mathrm{e}^{-\frac{1}{2}y^2}\,\mathrm{He}_{2p-3}(y), \tag{12a}$$

$$\omega_{2p-2}^{(1)}(y; k) = \frac{\mathrm{e}^{-\frac{1}{2}y^2}\,\mathrm{He}_{2p}(y)}{\mathrm{He}_{2p}(0)}, \tag{12b}$$

$$v_{2p-2}^{(1)}(y; k) = \frac{1}{\mathrm{He}_{2p}(0)} \int_y^\infty \mathrm{e}^{-\frac{1}{2}t^2}\,\mathrm{He}_{2p}(t) \sinh\left[k(y-t)\right] \mathrm{d}t + \gamma_{2p-2}\,\mathrm{e}^{-ky} - \frac{\beta_{2p-2}(k)}{k} \int_y^\infty \mathrm{e}^{-\frac{1}{2}t^2}\,\mathrm{He}_{2p-2}(t) \sinh\left(k(y-t)\right) \mathrm{d}t, \tag{12c}$$

$$w_{2p-2}^{(1)}(y; k) = \frac{-1}{\mathrm{He}_{2p}(0)} \int_y^\infty \mathrm{e}^{-\frac{1}{2}t^2}\,\mathrm{He}_{2p}(t) \cosh\left(k(y-t)\right) + \gamma_{2p-2}\,\mathrm{e}^{-ky} + k\beta_{2p-2} \int_y^\infty \mathrm{e}^{-\frac{1}{2}t^2}\,\mathrm{He}_{2p-4}(t) \cosh\left(k(y-t)\right) \mathrm{d}t, \tag{12d}$$

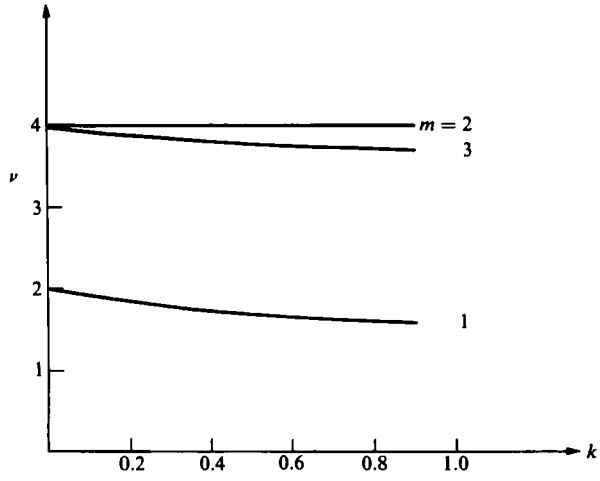

FIGURE 2. Eigenvalue branches of potential stagnation flow in (k, ν)-plane.

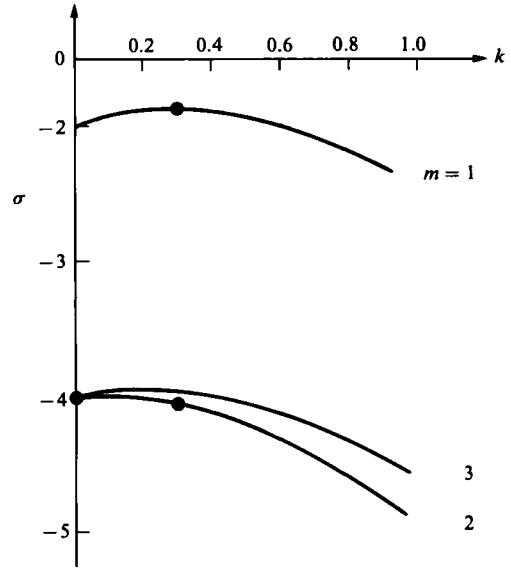

FIGURE 3. Eigenvalue branches of potential stagnation flow in (k, σ)-plane.

where $\mathrm{He}_l(y)$ denotes the Hermite polynomial of order l. The eigenfunctions have been normalized so that $\omega(0; k) = 1$,

$$\gamma_{2p-1}(k) = \frac{\int_0^\infty \mathrm{e}^{-\frac{1}{4}t^2+kt} D_{\nu_{2p-1}}(t)\,\mathrm{d}t}{2D_{\nu_{2p-1}}(0)}, \tag{13a}$$

$$\beta_{2p-2}(k) = \frac{k\int_0^\infty \mathrm{e}^{-\frac{1}{2}t^2-kt}\,\mathrm{He}_{2p-1}(t)\,\mathrm{d}t}{\mathrm{He}_{2p}(0)\int_0^\infty \mathrm{e}^{-\frac{1}{2}t^2-kt}\,\mathrm{He}_{2p-3}(t)\,\mathrm{d}t}, \tag{13b}$$

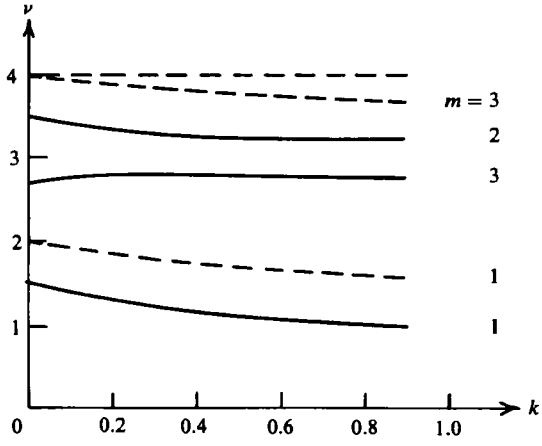

FIGURE 4. Eigenvalue branches of viscous stagnation flow (——) in (k, ν)-plane. Comparison with potential-stagnation-flow branches (– – –).

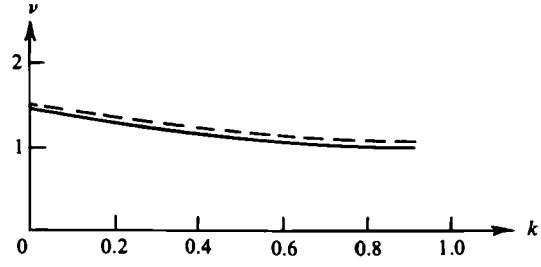

FIGURE 5. Comparison with numerical results of Wilson & Gladwell (1978): ——, single-mode approximation; – – –, numerical results.

$$\gamma_{2p-2}(k) = \frac{-k^{2p-2}\,\mathrm{He}_{2p-2}(0)\int_0^\infty \mathrm{e}^{-\frac{1}{2}t^2}\cosh(kt)\,\mathrm{d}t}{\mathrm{He}_{2p}(0)\int_0^\infty \mathrm{e}^{-\frac{1}{2}t^2-kt}\,\mathrm{He}_{2p-3}(t)\,\mathrm{d}t}. \tag{13c}$$

In (11) and (13a), it is implied that $\nu(k) \equiv \nu_{2p-1}(k)$. The adjoint eigenfunctions can be determined analytically by standard techniques (Morse & Feshbach 1953). (For further details, see Lyell 1982.)

3.2. *Linear stability of Hiemenz stagnation flow*

The trial-function vectors $\boldsymbol{U}_{nm}^{(j)}(y)$ appearing in (4) are chosen to be the eigenvectors $\boldsymbol{U}_m^{(j)}(y; nq)$ of potential stagnation flow evaluated at the wavenumber $k = nq$. Correspondingly, we select the adjoint trial-function vector to be $\bar{\boldsymbol{U}}_{nm}^{(j)}(y) = \bar{\boldsymbol{U}}_m^{(j)}(y; nq)$. For simplicity, we consider a class of motions for which $\hat{u}$ and $\hat{v}$ are even functions of z and $\hat{\omega}$ and $\hat{w}$ are odd functions. It is then straightforward to check that these symmetry properties are preserved under the nonlinear governing equations (3). Thus in the rest of the work, (4) is assumed to contain only eigenvectors with a (1) superscript. Henceforth, this superscript will be omitted.†

† However, it should be stressed that, in general, the Fourier series expansion (4) in z will be a linear combination of *both* sets of eigenvectors.

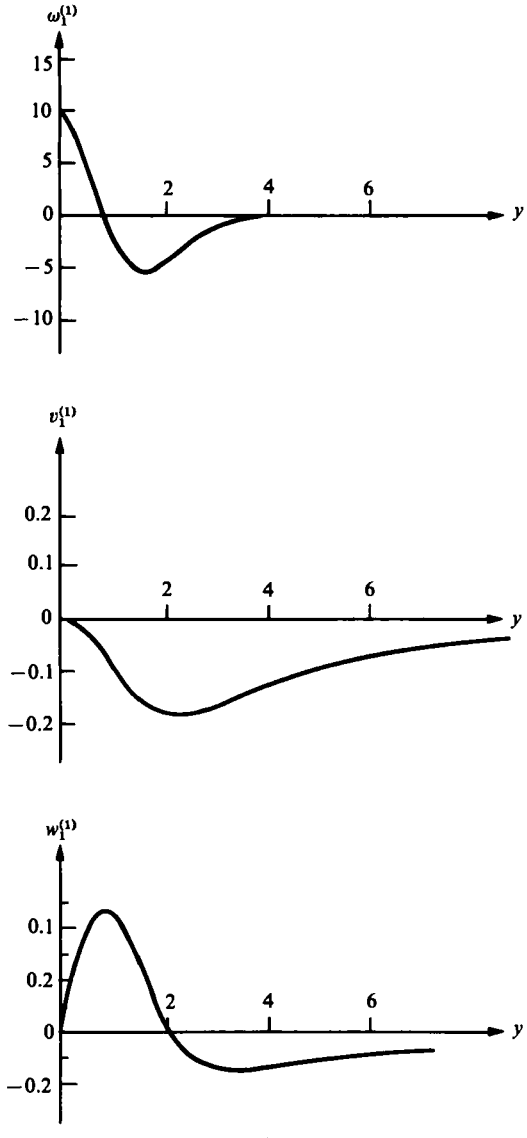

FIGURE 6. Potential-stagnation-flow eigenfunctions: first branch $m = 1$, $k = 0.30$.

The linear growth rates $\sigma_i(k)$ pertaining to viscous stagnation flow are given by the eigenvalues of the matrix $\{\alpha_{nm}\}$, n fixed, appearing in the amplitude equations (6). Leading-order Galerkin approximations can be obtained by considering single trial-function truncations for each branch. The resulting first three eigenvalues, $\nu_i(k) = -\sigma_i(k) - k^2$, $i = 1, 2, 3$, as well as their potential-flow counterparts, are displayed on figure 4. In both instances, there is an infinite number of eigenvalues which are all damped ($\nu > 0$, $\sigma < 0$). We note, however, that the decay rates $|\sigma|$ of Hiemenz flow are smaller than those of potential stagnation flow. Thus the simultaneous presence of mean-flow vorticity and streamline curvature is linearly destabilizing but the associated inviscid centrifugal instability mechanism is too weak to overcome viscous forces. In figure 5 our results for the least-damped batch are compared with the numerical values of Wilson & Gladwell (1978): the single-mode

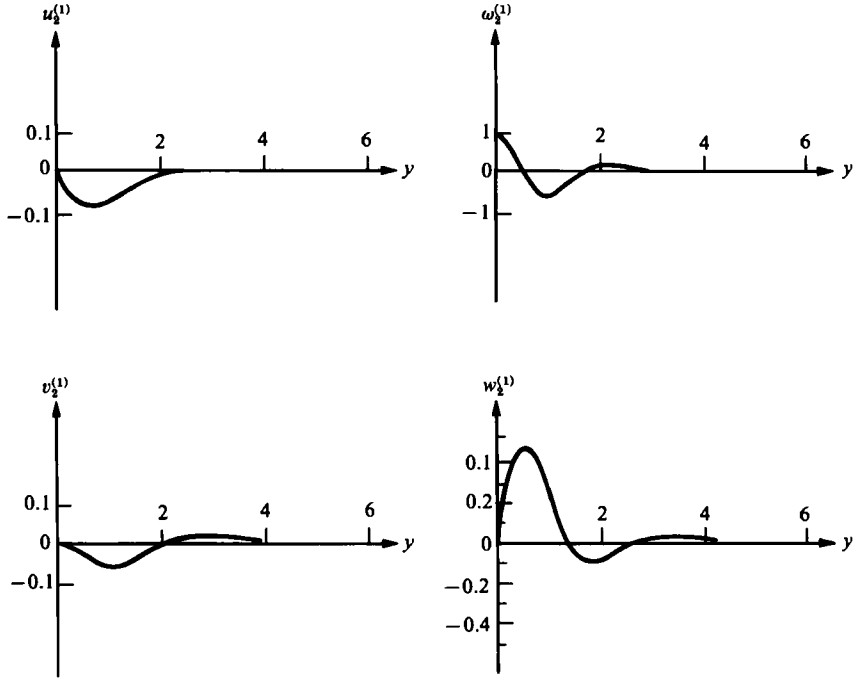

FIGURE 7. Potential-stagnation-flow eigenfunctions: second branch $m = 2$, $k = 0.30$.

approximation falls within 10% of the exact eigenvalue. Two-mode truncations performed at $k = 0.30$ are found to approach Wilson & Gladwell's results within 5%. Thus our choice of trial functions is seen to provide good estimates of the linear eigenvalues, even when the modal expansions are drastically truncated.

3.3. *Structure of the perturbation flow field*

Attention is now given to the perturbed flow field associated with potential stagnation flow. The eigenfunctions of the least-damped mode at $k = 0.30$ on the first branch $m = 1$ are displayed in figure 6. Note that odd-numbered branches are characterized by a zero streamwise velocity u and a vorticity vector aligned in the streamwise direction: they give rise to a purely two-dimensional fluctuating motion in the (y, z)-plane. The eigenfunctions of the second branch $m = 2$ at $k = 0.30$ are represented in figure 7. We note that, for both families, all variables decay exponentially at upstream infinity, thereby satisfying the same asymptotic boundary conditions as those derived in Wilson & Gladwell (1978). At zero wavenumber, the even-numbered modes correspond to a strictly two-dimensional vortical motion in the (u, v)-plane (see figure 8), whereas the odd-numbered modes represent a purely spanwise w-motion. Both types of perturbations represent possible mean-flow distortions of the basic two-dimensional stagnation flow. The mean of a flow quantity is here defined as being taken over one wavelength in the spanwise direction and may be time dependent. Eigenfunction shapes were found to be fairly insensitive to changes in k within the range $0.1 < k < 1.2$. Perturbation streamlines and lines of constant streamwise vorticity in the (y, z)-plane are illustrated in figures 9, 10, and 11 for the first three branches. The streamline plots clearly indicate that the perturbation field of each mode is composed of counter-rotating streamwise vortices periodically distributed in

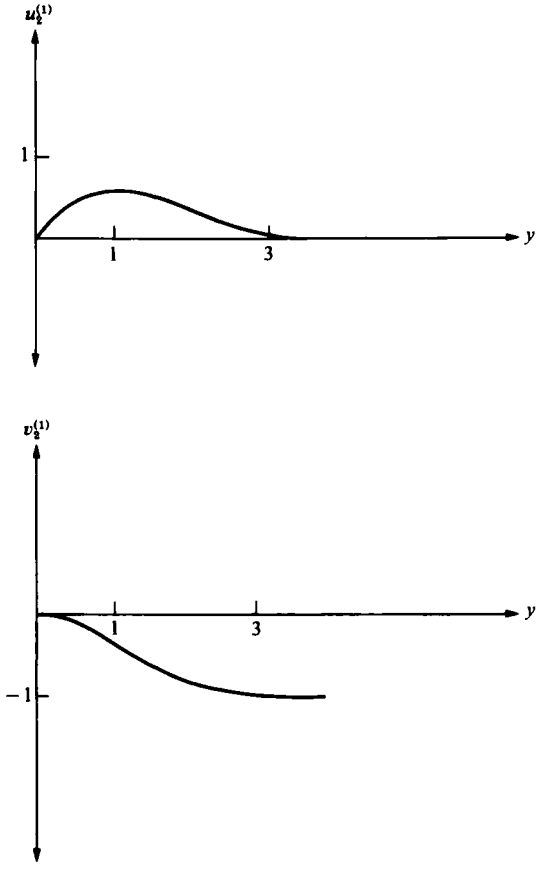

FIGURE 8. Potential-stagnation-flow eigenfunction: second branch $m = 2$, $k = 0$. Normalization condition changed to $\mathrm{d}u(0,0)/\mathrm{d}y = 1$.

the spanwise z-direction. According to the order of the mode, several layers of vortices may be stacked on top of each other in the upstream y-direction. Hence, whereas the first two odd modes $m = 1$ and $m = 3$ are composed of only one layer, the first even mode $m = 2$ is characterized by two layers. The number of layers increases monotonically with the modal index p but remains constant with spanwise wavenumber k along a given branch. There does not seem to exist any obvious relationship between the index p and the number of layers. The above discussion has been restricted to disturbances of class (1) in the sense of equations (7). Disturbances of class (2) have the same eigenvalues $\{\nu_m(k)\}$ as those of class (1), the associated eigenfunction vectors $\boldsymbol{U}_m^{(2)}(y;k)$ being related to $\boldsymbol{U}_m^{(1)}(y;k)$ by the transformation $\boldsymbol{U}_m^{(2)\,\mathrm{T}} = \{u_m^{(1)}, -\omega_m^{(1)}, v_m^{(1)}, -w_m^{(1)}\}$.

4. Nonlinear stability of viscous stagnation flow

In selecting a suitable truncation for the nonlinear study, it is first desirable to choose few enough modes so that the system of amplitude equations can be analysed in detail. Thus in this initial investigation of the nonlinear stability of Hiemenz flow we have not attempted to provide a quantitative picture of the finite-amplitude regime but rather we have sought to show that nonlinear interactions between a few

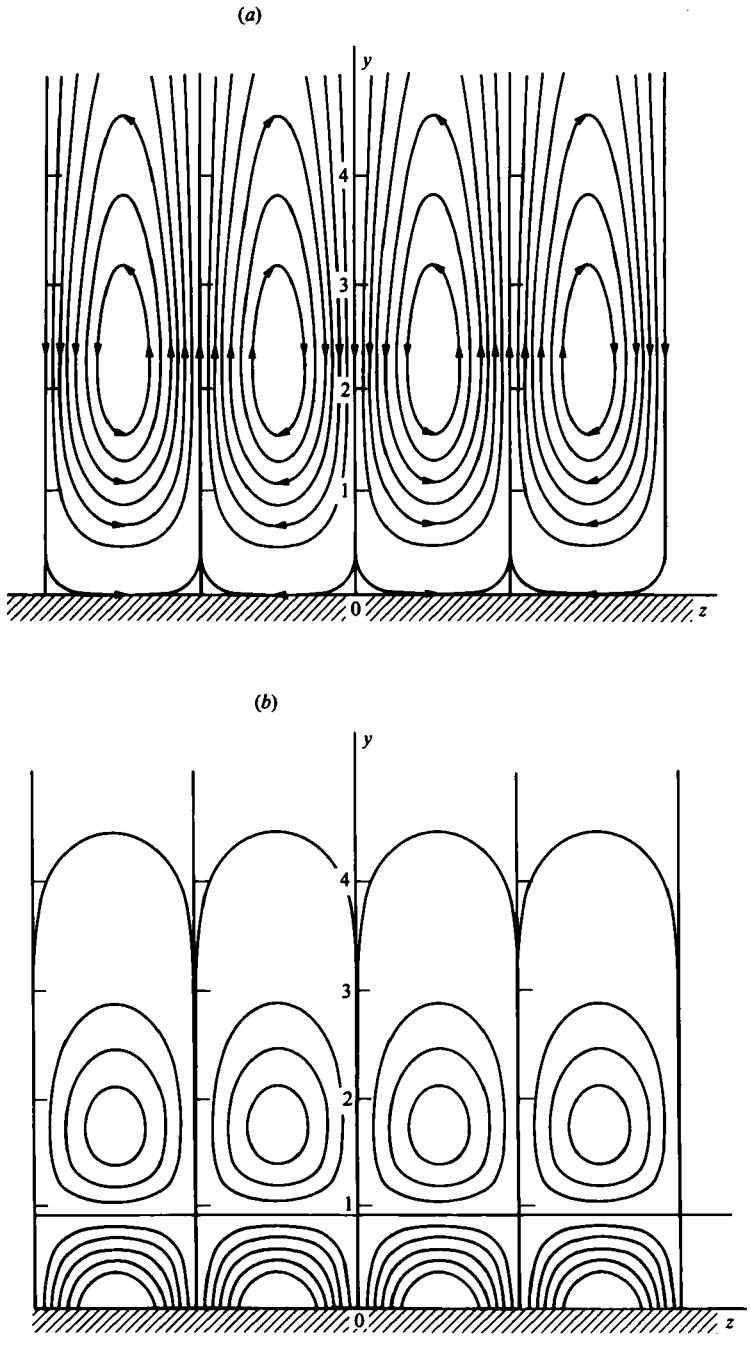

FIGURE 9. Perturbation streamlines (*a*) and constant-streamwise-vorticity contours (*b*): $m = 1$, $k = 0.30$.

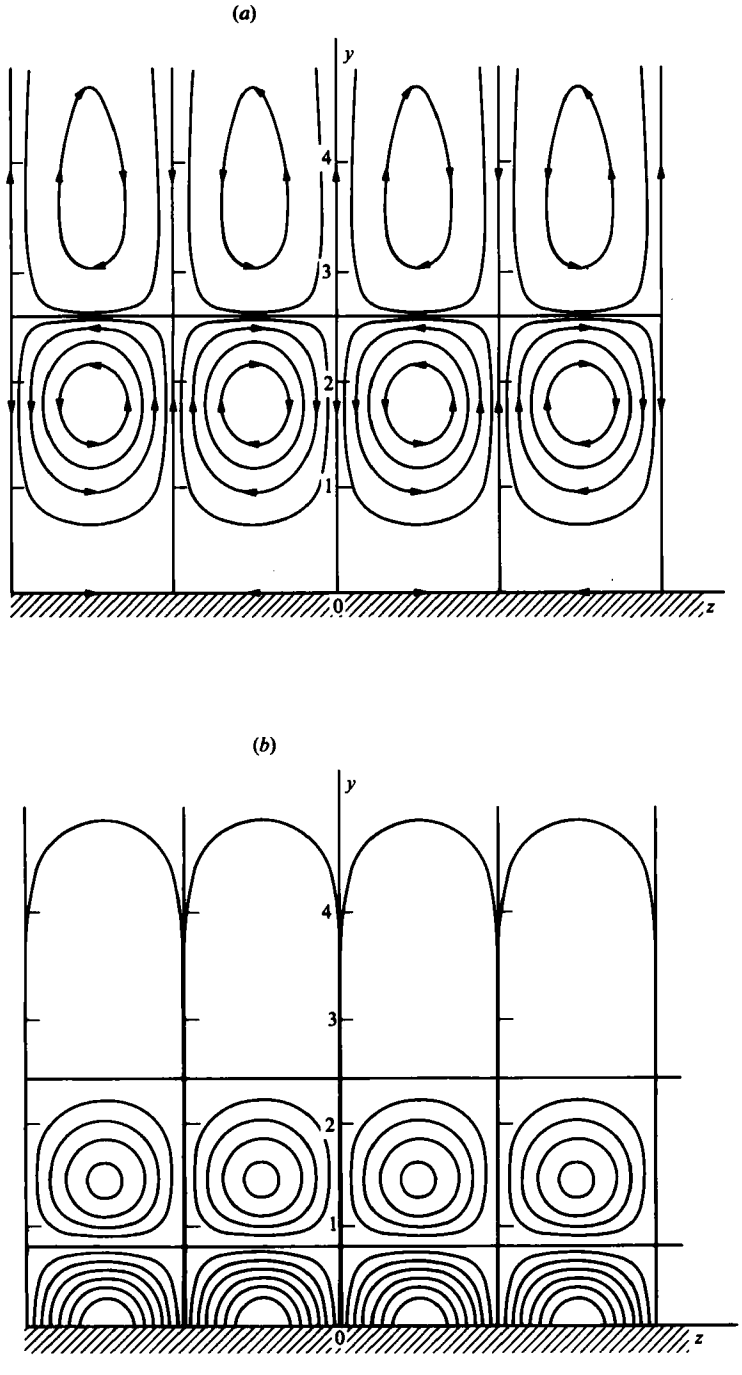

FIGURE 10. Perturbation streamlines (*a*) and constant-streamwise-vorticity contours (*b*): $m = 2$, $k = 0.30$.

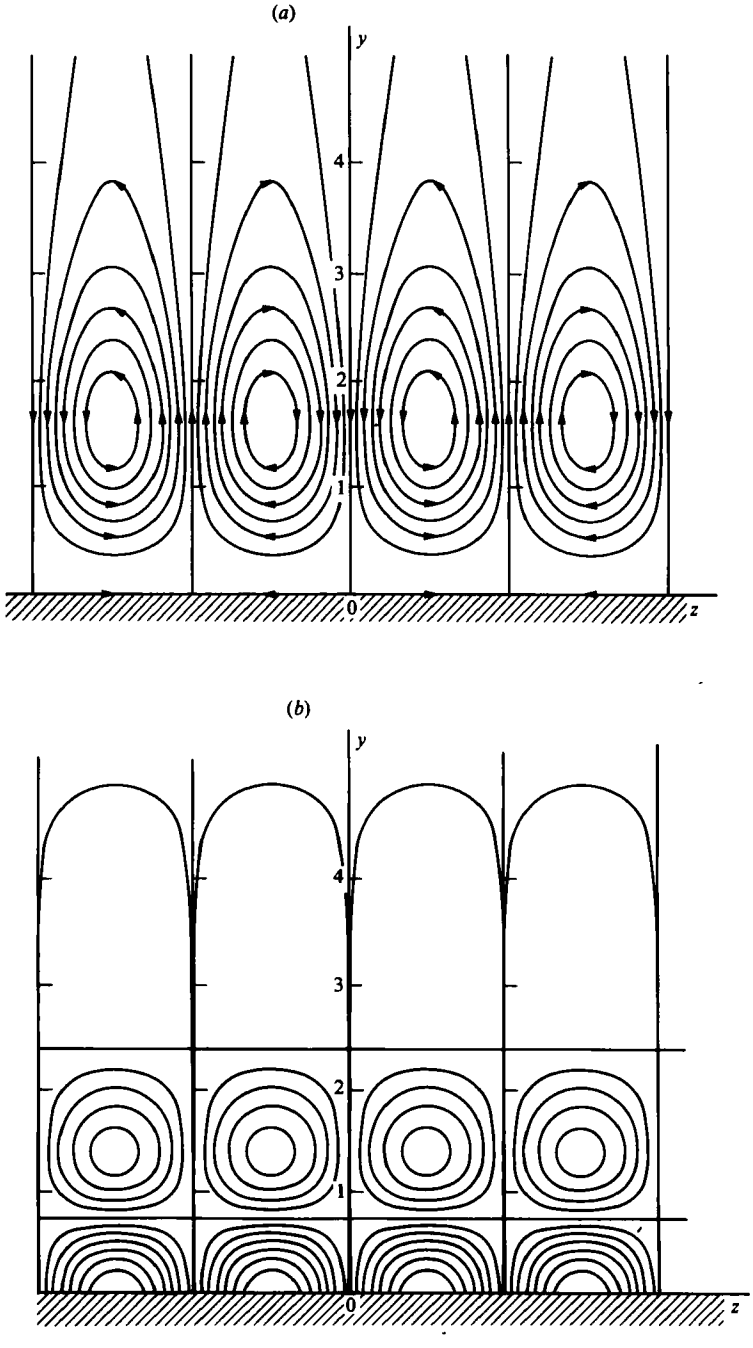

FIGURE 11. Perturbation streamlines (*a*) and constant-streamwise-vorticity contours (*b*): $m = 3$, $k = 0.30$.

modes can indeed lead to instability. The following three-mode decomposition has been selected:

$$\hat{u}(y,z,T) \approx A_{02}(T)\,u_{02}(y)+A_{12}(T)\,u_{12}(y)\cos(qz), \tag{14a}$$

$$\hat{\omega}(y,z,T) \approx \{A_{11}(T)\,\omega_{11}(y)+A_{12}(T)\,\omega_{12}(y)\}\sin(qz), \tag{14b}$$

$$\hat{v}(y,z,T) \approx A_{02}(T)\,v_{02}(y)+\{A_{11}(T)\,v_{11}(y)+A_{12}(T)\,v_{12}(y)\}\cos(qz), \tag{14c}$$

$$\hat{w}(y,z,T) \approx \{A_{11}(T)\,w_{11}(y)+A_{12}(T)\,w_{12}(y)\}\sin(qz). \tag{14d}$$

The spanwise wavenumber is taken to be the least damped according to linear theory: $q = 0.30$. All higher harmonics have been discarded. We have only retained the two leading three-dimensional modes $A_{11}(T)$ and $A_{12}(T)$ located on the first odd-numbered branch and even-numbered branch and the single least-damped two-dimensional mode $A_{02}(T)$. These disturbances are indicated by circles on the attenuation-*versus*-wavenumber diagram of figure 3. Following the procedure outlined in §2, one is led to the third-order system

$$\frac{\mathrm{d}A_{02}}{\mathrm{d}T} = -2.964A_{02}-1.197A_{02}^2-0.005A_{12}^2+0.006A_{11}\,A_{12}, \tag{15a}$$

$$\frac{\mathrm{d}A_{11}}{\mathrm{d}T} = -1.312A_{11}+0.268A_{12}-0.791A_{02}\,A_{11}-0.097A_{02}\,A_{12}, \tag{15b}$$

$$\frac{\mathrm{d}A_{12}}{\mathrm{d}T} = -3.407A_{12}-0.387A_{11}+1.171A_{02}\,A_{11}-1.458A_{02}\,A_{12}. \tag{15c}$$

This system possesses two critical points in the phase space (A_{11}, A_{12}, A_{02}) of solution trajectories. The origin is a stable node, as it should be, since it represents Hiemenz flow, which is stable to infinitesimal disturbances. The other critical point is at $(A_{11}, A_{12}, A_{02}) = (0, 0, -2.476)$ and is found to be an unstable spiral: in its immediate vicinity, the phase flow is expanding in the direction of decreasing A_{02} and undergoing a spiralling motion in the plane $A_{02} = -2.476$. Solution trajectories located below the plane $A_{02} = -2.476$ become unbounded and therefore give rise to amplified disturbances. Initial conditions corresponding to points in phase space such that A_{02} is positive only give rise to damped disturbances. Trajectories starting in the region of phase space delimited by the two planes $A_{02} = 0$ and $A_{02} = -2.476$ either converge to the origin or become unbounded, the nature of the motion varying from point to point. The destabilizing effect of the two-dimensional mode A_{02} is further confirmed by two-mode truncation models which may easily be generated from (15). The structure of phase space for the (A_{02}, A_{11}) and (A_{02}, A_{12}) bi-modal interaction systems is shown in figures 12 and 13 respectively. In both cases, there is a threshold curve in phase space separating trajectories which are attracted to the origin from those which are unbounded. For amplitudes of the two-dimensional mode such that $A_{02} < -2.476$, disturbances always become amplified and the linearly stable Hiemenz flow is destabilized.

We do not mean to imply that Hiemenz flow can be nonlinearly destabilized only if a two-dimensional mode of sufficiently large initial amplitude is present. For instance, the study of a two-mode truncation (A_{12}, A_{21}) involving only three-dimensional disturbances has indicated finite-amplitude instability above a threshold value of the order of 10 (Lyell 1982).

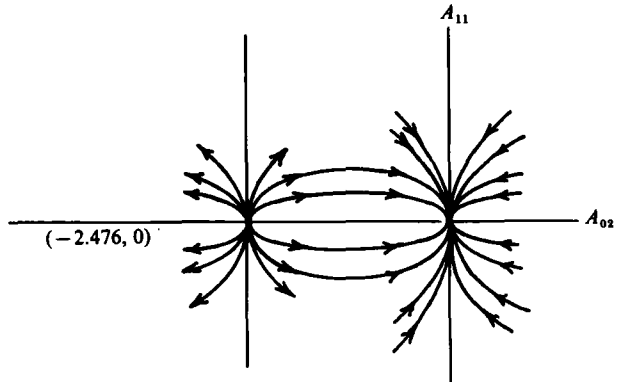

FIGURE 12. Two-mode truncation. Phase flow in plane (A_{02}, A_{11}).

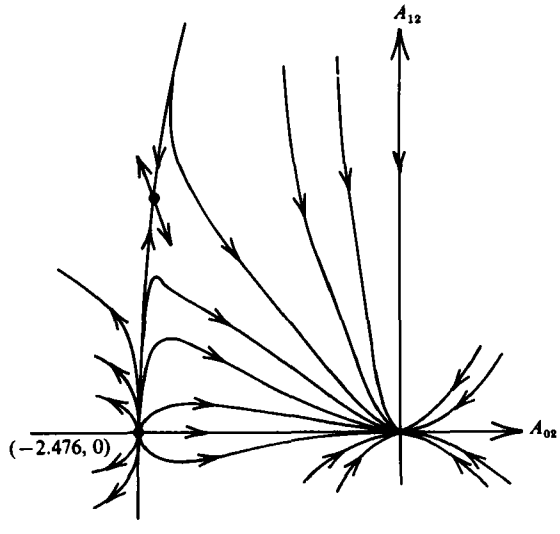

FIGURE 13. Two-mode truncation. Phase flow in plane (A_{02}, A_{12}).

5. Discussion and conclusions

In the linear stability analysis of Hiemenz flow we have shown that the eigenvalues and eigenfunctions calculated by Wilson & Gladwell (1978) constitute the least-damped mode of an infinite number of modes, all of which are attenuated in time. Each mode corresponds, in the terminology of Morkovin (1979), to a vortex module composed of a specific number of streamwise vortices stacked in the upstream direction, the number of layers increasing with the order of the mode. The presence of concave streamline curvature and mean-flow vorticity had led Görtler (1955) and Hämmerlin (1955) to suspect that Hiemenz flow is centrifugally unstable. According to our comparison of the attenuation rates prevailing in potential stagnation flow and viscous stagnation flow, mean-flow vorticity indeed leads to a relative destabilization by centrifugal forces but viscous effects are too strong to give rise to linear instability. We note that the vortical structures exhibited in the flow-visualization studies of Hodson & Nagib (1975) and Sadeh & Brauer (1980) are fully consistent with the three-dimensional perturbed flow field of the least-damped branch $m = 1$. Such

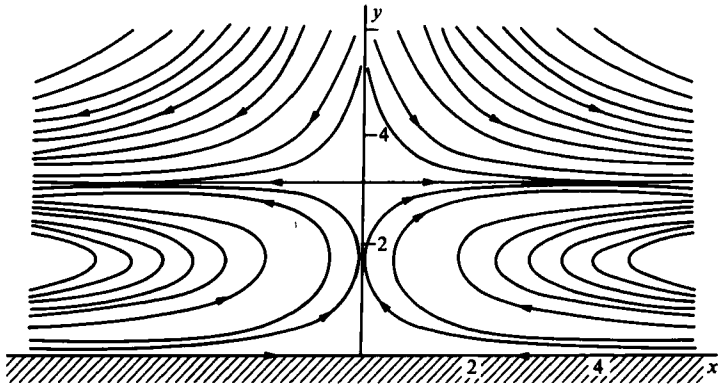

FIGURE 14. Two-dimensional mean flow obtained by superposition of Hiemenz flow and two-dimensional mode $m = 2$, $k = 0$, at instability threshold $A_{02} = -2.476$.

patterns are also in agreement with the vortex-module concept of Morkovin (1979).

Highly truncated Galerkin expansions in terms of the eigenfunctions of potential stagnation flow have shown that Hiemenz flow can be nonlinearly destabilized if the level of two- or three-dimensional disturbances exceeds a certain threshold value. We note that the magnitude of the threshold is large enough to lead to flow reversal in the immediate vicinity of the wall, as shown by the two-dimensional mean-flow streamlines of figure 14. However, it is unlikely that such a pattern will be observed in practice, as it is unstable. Since our models do not display a stable critical point, other than the origin, the ultimate finite-amplitude state above threshold is beyond the scope of this analysis. Nonlinear interactions have so far been limited to two or three modes and this conclusion can only be viewed as qualitative. The modes that have been retained are, however, those which are least attenuated according to linear theory and can be most easily destabilized.

In the experiments of Hodson & Nagib (1975), the only ones to be discussed here, controlled free-stream disturbances were provided by the wakes shed from a periodic array of rods placed at a certain fixed distance upstream from a circular cylinder. The structure of the stagnation flow field was then observed for various rod Reynolds numbers. At low Reynolds numbers, of the order of 30, steady counter-rotating vortices were found to characterize the response to the steady upstream spanwise periodic wakes. In all cases, these experiments indicated that the secondary flow could be observed only if the strength of the wakes exceeded a certain threshold level. At higher rod Reynolds numbers, of the order of 90, the steady upstream wakes gave way to laminar Kármán vortex streets and the secondary vortices became unsteady as a result of the time-periodic excitation.

The existence of a theoretical threshold agrees with the experimental observations in the steady regime. We note, however, that in the theory the threshold pertains to the level of perturbations at $t = 0$, in an initial-value problem, where all normal modes are exponentially decaying far upstream. In experimental studies, disturbances are forced into the flow from upstream and experience algebraic decay or growth as they penetrate the stagnation-flow region. The precise process by which such forced disturbances might trigger an instability of the normal modes remains to be investigated.

We are very grateful to Professor R. F. Blackwelder for introducing us to this problem and for helpful discussions. We also wish to thank Professor L. G. Redekopp for many useful suggestions. This work was supported by the Air Force Office of Scientific Research Contracts F49620-78-0060 and F49620-82-K-0019.

REFERENCES

COLAK-ANTIC, P. 1971 Visuelle Untersuchungen von Langswirbeln im Staupunktgebiet eines Kreiszylinders bei turbulenter Anströmung. *D.L.R. Mitteilung* 71-13, Bericht über die DGLR-Fachausschuss-Sitzung, Laminare und Turbulente Grenzschichtung, p. 194. Göttingen.

DIPRIMA, R. 1967 Vector eigenfunction expansions for the growth of Taylor vortices in the flow between rotating cylinders. In *Nonlinear Partial Differential Equations* (ed. W. F. Ames), p. 19. Academic.

FINLAYSON, B. 1972 *The Method of Weighted Residuals and Variational Principles.* Academic.

GÖRTLER, H. 1955 Dreidimensionale Instabilität der ebenen Staupunkt-Strömung gegenüber wirbelartigen Störungen. In *Fifty Years of Boundary Layer Research* (ed. H. Görtler & W. Tollmien), p. 304. Vieweg und Sohn.

HALL, P. 1982 Taylor–Görtler vortices in fully developed or boundary-layer flows: linear theory. *J. Fluid Mech.* **124**, 475.

HALL, P. 1983 The linear development of Görtler vortices in growing boundary layers. *J. Fluid Mech.* **130**, 41.

HÄMMERLIN, G. 1955 Zur Instabilitätstheorie der ebenen Staupunktströmung. In *Fifty Years of Boundary Layer Research* (ed. H. Görtler & W. Tollmien), p. 315. Vieweg und Sohn, Braunschweig.

HASSLER, H. 1971 Hitzdrahtmessungen von Langswirbelartigen Instabilitätserscheinungen im Staupunktgebiet eines Kreiszylinders in turbulenter Anströmung. *D.L.R. Mitteilung* 71-13, Bericht über die DGLR-Fachausschuss-Sitzung, Laminare und Turbulente Grenzschichtung, p. 221. Göttingen.

HODSON, P. & NAGIB, H. 1975 Longitudinal vortices induced in a stagnation region by wakes – their incipient formation and effects on heat transfer from cylinders. *IIT Fluids and Heat Transfer Rep.* R75-2.

IIDA, S. 1978 Nonlinear stability of a two-dimensional stagnation flow. *Bull. Japan Soc. Mech. Engng* **21**, 992.

LYELL, M. J. 1982 The nonlinear stability of two fluid flows: three-dimensional plane stagnation flow and two-dimensional jets. Ph.D. thesis, University of Southern California.

MORKOVIN, M. 1979 On the question of instabilities upstream of cylindrical bodies. *IIT Fluids and Heat Transfer Rep.* R79-3.

MORSE, P. M. & FESHBACH, H. 1953 *Methods of Theoretical Physics.* McGraw-Hill.

PIERCY, N. & RICHARDSON, E. 1928 The variation of velocity with amplitude close to the surface of the cylinder moving through a viscous fluid. *Phil. Mag.* **6**, 970.

SADEH, W. & BRAUER, H. 1980 A visual investigation of turbulence in stagnation flow about a circular cylinder. *J. Fluid Mech.* **99**, 53.

SADEH, W., SUTERA, S. & MAEDER, P. 1970 An investigation of vorticity amplification in stagnation flow. *Z. angew. Math. Phys.* **21**, 717.

SCHLICHTING, H. 1979 *Boundary Layer Theory.* McGraw-Hill.

STUART, J. T. 1960 On the nonlinear mechanics of wave disturbances in stable and unstable parallel flows. Part 1. *J. Fluid Mech.* **9**, 353.

WATSON, J. 1960 On the nonlinear mechanics of wave disturbances in stable and unstable parallel flows. Part 2. *J. Fluid Mech.* **9**, 371.

WILSON, S. & GLADWELL, I. 1978 The stability of a two-dimensional stagnation flow to three-dimensional disturbances. *J. Fluid Mech.* **84**, 517.